weights. A vertex is *free* if it is not an endvertex of any edge in $M$. A graph $G = (V, E)$ is called *bipartite* if there is a subset $V^+$ of $V$ such that every edge has one endvertex in $V^+$ and the other in $V^- = V - V^+$. Such a bipartite graph is often denoted by $G = (V^+, V^-, E)$. Let $M$ be a matching on a bipartite graph $G = (V^+, V^-, E)$ or a network $N = (G = (V^+, V^-, E); b)$. $M$ is *perfect* if $|M| = |V^+| = |V^-|$. A perfect matching of $N$ of minimum weight is an *optimal assignment* of $N$. A path in a directed graph $G = (V, E)$ or a network $N = (G = (V, E); b)$ from vertex $w_1$ to $w_p$ is a list of vertices $P = [w_1, w_2, \cdots, w_p]$ such that every $e_i = [w_i, w_{i+1}]$ is a directed edge for $i = 1, 2, \cdots, p-1$. The *length* of $P$ is the sum of its edge weights. A *shortest path* of $N$ from $w_1$ to $w_p$ is a path of minimum length from $w_1$ to $w_p$. The *distance* from $w_1$ to $w_p$ is the length of a shortest path from $w_1$ to $w_p$.

### Acknowledgment

The authors would like to express their sincere gratitude to Prof. K. Murota of the University of Tokyo, and Prof. K. Tamura of Sophia University for valuable comments and discussion.

### References

[1] T. Asano, K. Yoshikawa, and S. Suzuki, "A network-theoretic approach to the design of a precompensator for multivariable adaptive control," Tech. Rep. (87-01), Dep. Mech. Eng., Sophia Univ., 1987.
[2] S. W. Chan and G. C. Goodwin, "On the role of the interactor matrix in multiinput-multioutput adaptive control," *IEEE Trans. Automat. Contr.*, vol. AC-27, pp. 713-714, 1982.
[3] L. Dugard and J. M. Dion, "Direct adaptive control for linear multivariable systems," *Int. J. Contr.*, vol. 42, pp. 1251-1281, 1985.
[4] L. Dugard, G. C. Goodwin, and C. E. deSouza, "Prior knowledge in model reference adaptive control of multiinput multioutput systems," *IEEE Trans. Automat. Contr.*, vol. AC-29, pp. 761-764, 1984.
[5] H. Elliott and W. A. Wolovich, "A parameter adaptive control structure for linear multivariable systems," *IEEE Trans. Automat. Contr.*, vol. AC-27, pp. 340-352, 1982.
[6] ——, "Parameterization issues in multivariable adaptive control," *Automatica*, vol. 20, pp. 533-546, 1984.
[7] M. L. Fredman and R. E. Tarjan, "Fibonacci heaps and their uses in improved network optimization algorithms," in *Proc. 25th Annu. IEEE Symp. Foundations Comput. Sci.*, Singer Islands, 1984, pp. 338-346.
[8] G. C. Goodwin and R. S. Long, "Generalization of results on multivariable adaptive control," *IEEE Trans. Automat. Contr.*, vol. AC-25, pp. 1241-1245, 1980.
[9] R. Johansson, "Parametric models for linear multivariable systems for adaptive control," *IEEE Trans. Automat. Contr.*, vol. AC-32, pp. 303-313, 1987.
[10] E. L. Lawler, *Combinatorial Optimization: Networks and Matroids*. New York: Holt, Rinehart and Winston, 1976.
[11] C. H. Papadimitriou and K. Steiglitz, *Combinatorial Optimization: Algorithms and Complexity*. Englewood Cliffs, NJ: Prentice-Hall, 1982.
[12] R. P. Singh and K. S. Narendra, "Prior information in the design of multivariable adaptive controller," *IEEE Trans. Automat. Contr.*, vol. AC-29, pp. 1108-1111, 1984.
[13] K. Tamura and W. Kase, "A design of a pre-compensation for linear multivariable systems and its application to discrete-time indirect MRACS," Dep. Mech. Eng., Sophia Univ., 1987, unpublished note.
[14] R. E. Tarjan, "Data structures and network algorithms," CBMS-NFS Regional Conf. Series Appl. Math. 44, SIAM, Philadelphia, PA, 1983.
[15] W. A. Wolovich and P. L. Falb, "Invariants and canonical forms under dynamic compensation," *SIAM J. Contr. Optimiz.*, vol. 14, pp. 996-1008, 1976.

# Contact Instability of the Direct Drive Robot when Constrained by a Rigid Environment

H. KAZEROONI

***Abstract*—Robot manipulations require mechanical interaction with the environment (i.e., the object being manipulated) which can constrain the robot endpoint in some or all directions. A sufficient condition for the stability of robot manipulators in constrained maneuvers is derived in the work presented here. Attention is focused on the class of direct drive robots whose rigid links dominate the robot's dynamic behavior; compared to the robot, the environment is assumed to be infinitely rigid. The stability of the manipulator-environment system is investigated, and a bound for stable manipulation is determined. This bound is verified via simulation and experiment on the Minnesota direct drive robot.**

Manuscript received March 3, 1988; revised October 21, 1988 and May 15, 1989. Paper recommended by Past Associate Editor, T. J. Tarn.

The author is with the Mechanical Engineering Department, University of Minnesota, Minneapolis, MN 55455.

IEEE Log Number 9034499.

## I. Introduction

Both fast motion in unconstrained space and mechanical interaction with the environment (i.e., the object being manipulated) are required in most robotic manufacturing tasks. Robotic assembly is an example of such a task where the robot must follow a trajectory when unconstrained by the environment, but during the insertion process, the robot must comply with the environmental constraints. Robotic deburring [6] is another example of such a task where the interaction force[1] must be accommodated rather than resisted.

Two methods are suggested for implementing compliant motion [24]. The first method controls force and position in a nonconflicting way [15]-[18], [23]: force is commanded along those directions constrained by the environment, while position is commanded along those directions in which the manipulator is free to move. The second method develops a relationship between the interaction force and the manipulator position [4], [5], [10]-[13], [19]. By controlling the manipulator position and specifying its relationship with the interaction force, a designer ensures that the manipulator can maneuver in a constrained space while maintaining appropriate contact force. This note analyzes the stability of the robot-environment system when the second method is employed to control robot compliancy. A sufficient condition for system stability is derived analytically and verified experimentally on a direct drive robot arm. References [5] and [11]-[13] give some preliminary results on the stability of robotic constrained maneuvers. A stability analysis for linear, single-degree-of-freedom systems is discussed in [1] and [2].

## II. Unconstrained Analysis

The dynamic behavior of direct drive robots with $n$ degrees of freedom is expressed by

$$M(\theta)\ddot{\theta} + C(\theta, \dot{\theta}) = \tau - J^T f \tag{1}$$

where $\ddot{\theta}, \dot{\theta}, \theta$ are vectors containing the joints' accelerations, velocities, and positions; $M(\theta)$ is the inertia matrix; $C(\theta, \dot{\theta})$ is the vector representing the coriolis, centrifugal, and gravity forces; $\tau$ is the vector of joint torques; $J^T$ is the Jacobian transpose matrix; and $f$ is the vector of external forces applied at the robot endpoint [3]. Trajectory control of the manipulator is performed by a digital implementation of a feedforward torque controller, which torque is given by

$$\tau = K_p(\theta_d - \theta) + K_v(\dot{\theta}_d - \dot{\theta}) + \hat{M}(\theta_d)\ddot{\theta}_d + \hat{C}(\theta_d, \dot{\theta}_d) \tag{2}$$

where $\tau$ is the vector of joint torques; $(\theta_d - \theta)$ is the error between the command position, $\theta_d$, and the actual position, $\theta$; $(\dot{\theta}_d - \dot{\theta})$ is the error between the respective velocities; $K_p$ is an $n \times n$ matrix containing the position gains; $K_v$ is an $n \times n$ matrix containing the velocity gains; $\hat{M}(\theta_d)$ and $\hat{C}(\theta_d, \dot{\theta}_d)$, which can be found experimentally or analytically, are educated guesses for $M(\theta)$ and $C(\theta, \dot{\theta})$. The nonlinear feedforward terms, $\hat{M}(\theta_d)$ and $\hat{C}(\theta_d, \dot{\theta}_d)$, cancel the nonlinear effects of $M(\theta)$ and $C(\theta, \dot{\theta})$ in the robot's dynamics and result in a nearly uncoupled linear system. (The feedforward controller and robot dynamics are shown in Fig. 1.) In feedforward torque control, the robot trajectory is specified in joint coordinates, and the joint positions, velocities, and accelerations for a given trajectory are computed and stored before the trajectory is executed. The $\text{kin}(\cdot)$ operator in the diagram represents the forward kinematics, while $\text{kin}^{-1}(\cdot)$ represents the inverse kinematics. When the trajectory is specified in Cartesian space as a function of time, $e(t)$, inverse kinematics and numerical differentiation transform it into the joint

[1] In this note, "force" implies force and torque, and "position" implies position and orientation.

0018-9286/90/0600-0710$01.00 

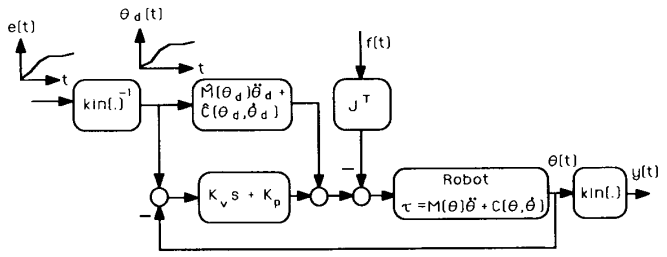


Fig. 1. The block diagram of the robot trajectory controller [20].

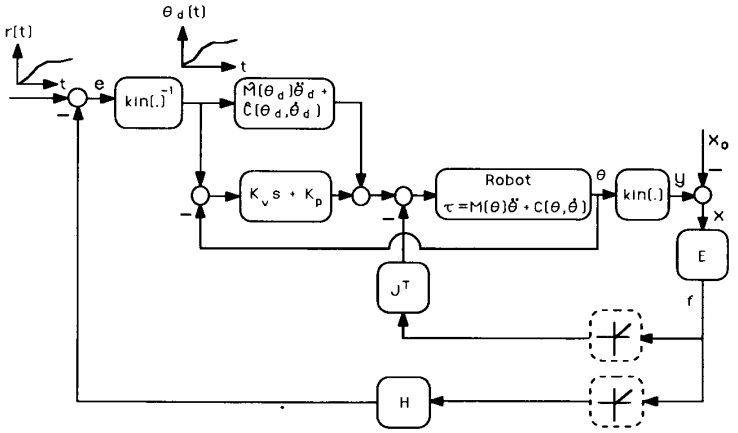


Fig. 2. In constrained maneuvers, the contact force, $f$, affects the robot via two feedback loops.

space, $\theta_d(t)$.

$$\theta_d(t) = \text{kin}^{-1}[e(t)] \tag{3}$$

$$y(t) = \text{kin}[\theta(t)]. \tag{4}$$

The nonlinear control law of (2) is chosen because the inertia and coriolis terms can be computed and stored. During the trajectory execution, these terms are added to the error terms to compute the joint torques. The chief advantage of this approach is that only a modest amount of computation must be performed in real time and the sampling time is correspondingly reduced.

Although computationally efficient, feedforward torque control does not achieve perfect uncoupling of each joint. Using (1) and (2) and assuming that $\hat{C}(\theta_d, \dot{\theta}_d) \approx C(\theta, \dot{\theta})$ and $\hat{M}(\theta_d) \approx M(\theta)$, a differential equation in terms of the joint accelerations is obtained:

$$J^T f = K_p(\theta_d - \theta) + K_v(\dot{\theta}_d - \dot{\theta}) + M(\theta)(\ddot{\theta}_d - \ddot{\theta}) \tag{5}$$

where $M(\theta)$ is a symmetric, positive definite matrix whose inverse exists for all robot configurations, $\theta$. Despite the assumption that the robot dynamics are accurately known, the joints are not perfectly uncoupled, and the degree of coupling varies as a function of the robot configuration. If $K_p$ and $K_v$ are chosen as positive definite matrices, the robot dynamic behavior will be $L_2$ stable, and $(\theta_d - \theta)$ will be an $L_2$ bounded quantity even in the presence of nonzero, but bounded, uncertainties in computing $\hat{C}(\theta_d, \dot{\theta}_d)$ and $\hat{M}(\theta_d)$ [20].

## III. Constrained Analysis

Fig. 2 shows the robot interacting with the environment where the robot compliancy is created by an $H$ compensator. The environment produces a force, $f$, which is expressed in the global Cartesian coordinate frame as $f = E(x)$. In many applications, $f$ may be zero if $x$ is negative. For example, in the grinding of a surface, if positive $f_i$ is "pushing" and negative $f_i$ is "pulling," the robot and the environment contact each other only along those directions where $f_i > 0$ for $i = 1, \cdots, n$. In some applications, such as turning a bolt, the interaction force can be either positive or negative, meaning that the interaction torque can be either clockwise or counterclockwise. The nonlinear discriminator block diagram in Fig. 2 is drawn with a dashed line to represent the above concept; the block is present only when the interaction forces are compressive. Reference [10] represents $(Is^2 + Ds + K)$ for the environment dynamics, $E$, where $I$, $D$, and $K$ are symmetric matrices and $s = j\omega$ [14]. $I$ is the positive definite inertia matrix, and $D$ and $K$ are the positive semidefinite damping matrix and the stiffness matrix.

Although the trajectory controller operates in the manipulator joint space, $H$ is implemented as a transfer function matrix. $H$ accepts the Cartesian force and produces a signal representing a Cartesian displacement which subtracts from the commanded trajectory such that $e(t) = r(t) - Hf(t)$. The input command vector, $r$, is used differently for the two types of maneuvers: as a command to specify the input trajectory in unconstrained maneuvers, and as a command to control force in constrained maneuvers. We do not assign any set point for force as we do in admittance control [15]–[18], [23]. This method is referred to as Impedance Control [4], [10] because it accepts a position vector as input and it returns a force vector as output. There is no hardware or software switch in the control system when the robot travels between unconstrained space and constrained space. When the robot encounters the environment, the feedback loop on the contact force closes naturally. The contact force is shaped by the robot dynamics and the designers' choice of $H$. Depending on the task, $H$ can take on various values in different directions. A small $H$ generates a stiff robot, and a large $H$ results in a compliant robot [7]. However, $H$ cannot be arbitrarily large; the stability of the closed-loop system of Fig. 2 must be guaranteed.

When the robot contacts an infinitely stiff and stationary environment, the environment dictates the robot's position: in the constrained directions, the environment deflection, $x$, is zero and the robot position is the same as the environment position. In this analysis, the robot endpoint is assumed to be constrained by the environment in all directions; this represents the "worst" robot maneuver. Instability in this worst case is characterized by the unbounded oscillations of the contact forces while

$\theta$ remains a bounded quantity. The above are reflected in the following two equations:

$$\text{kin}[\theta(t)] = x_0 \tag{6}$$

$$\dot{\theta}(t) = \ddot{\theta}(t) = 0. \tag{7}$$

Substituting $\theta_d$, $\theta$, $\dot{\theta}(t)$, and $\ddot{\theta}(t)$ from (3), (6), and (7) into (5) and replacing $e$ with $(r - H^*\{f\})$ results in (8) where $H^*\{f\}$ implies the convolution of the impulse response of $H$ and $f$.

$$f = J^{-T}K_p\,\text{kin}^{-1}(r - H^*\{f\}) - J^{-T}K_p\,\text{kin}^{-1}(x_0) + J^{-T}K_v(\dot{\theta}_d) + J^{-T}M(\theta)\ddot{\theta}_d. \tag{8}$$

When the robot is not in contact with the environment (i.e., the outer feedback loops in Fig. 2 do not exist), the position of the robot endpoint is governed by (5). When the robot is in contact with the environment, the contact force follows $r$ according to (8). If the trajectory command, $r$, extends a small distance beyond the solid environment, $\text{kin}^{-1}$ can be replaced by $J^{-1}$ and (8) can be rewritten as

$$f = J^{-T}K_pJ^{-1}(r - H^*\{f\} - x_0) + J^{-T}K_v(\dot{\theta}_d) + J^{-T}M(\theta)\ddot{\theta}_d. \tag{9}$$

Since the environment is infinitely stiff, $E$ cannot be assumed to be an $L_2$ stable operator. This prevents substituting for $f$ (via the operator $E$ as a function of $x$ or $\theta$) in (9). Instead, $f$ is treated as the test parameter for the closed-loop stability; if $f$ is bounded in the $L_2$ sense, then the system will be stable. In the case of finite $E$, one can substitute for $f$, and an equation similar to (5) can be obtained for stability analysis. The truncated $L_2$ norm[2] of (9) is written as

$$\|f\|_{T2} \le \sigma_{\max}(J^{-T}K_pJ^{-1})\,\|H^*\{f\}\|_{T2} + \left\|J^{-T}K_pJ^{-1}(r - x_0)\right\|_{T2} + \left\|J^{-T}K_v(\dot{\theta}_d) + J^{-T}M(\theta)\ddot{\theta}_d\right\|_{T2}. \tag{10}$$

Since $\theta$ is dictated by the environment, $M(\theta)$ in (9) is a function of $X_0$ and consequently will be bounded. Since $r$, $x_0$, $\theta_d$, and $M(\theta)$ are bounded quantities, then the last two norms of inequality (10) will be bounded by a positive scalar, $\beta$, and inequality (10) can be written as

$$\|f\|_{T2} \le \sigma_{\max}(J^{-T}K_pJ^{-1})\,\|H^*\{f\}\|_{T2} + \beta. \tag{11}$$

$\|H^*\{f\}\|_{T2}$ can be replaced with $\sigma_{\max}(Q)\|f\|_{T2}$ where $\sigma_{\max}(Q)$ is the maximum singular value[3] of $Q$ and $Q$ is a matrix whose entry $(ij)$ is given by $(Q)_{ij} = \sup_\omega |H(j\omega)_{ij}|$. The closed-loop system of Fig. 2 is $L_2$ stable ($f$ is $L_2$ bounded) if inequality (12) is satisfied over the commanded trajectory.

$$\sigma_{\max}(J^{-T}K_pJ^{-1})\sigma_{\max}(Q) < 1 \tag{12}$$

or

$$\sigma_{\max}(Q) < \frac{1}{\sigma_{\max}(J^{-T}K_pJ^{-1})} \qquad \text{(over the commanded trajectory)}. \tag{13}$$

Equivalently, one can satisfy inequality (14).

$$\sigma_{\max}(Q) < \text{infimum of } \sigma_{\min}(JK_p^{-1}J^T) \qquad \text{(over the commanded trajectory)}. \tag{14}$$

[2]The $L_2$-norm of an $n \times 1$ vector function $f(t)$ is defined as [21], [22]

$$\|f\|_2 = \left[\int_0^\infty |f(t)|^2\,dt\right]^{1/2}$$

where $|f(t)|$ is the Euclidean norm evaluated at a given time $t$. If $\|f\|_2 \le \infty$, then we say that $f \in L_2^n$. For functions that may grow unboundedly, a truncated $L_2$-norm is defined

$$\|f\|_{T2} = \|f(t)\|_2, \qquad 0 \le t < T.$$

[3]The maximum singular value of a matrix $H$, $\sigma_{\max}(H)$ is defined as

$$\sigma_{\max}(H) = \max \frac{|Hz|}{|z|}, \qquad z = 0.$$

Fig. 3. The experimental direct drive robot.

The minimum singular value of $(JK_p^{-1}J^T)$ must be calculated at each point in the commanded trajectory. The infimum is the lowest of all the minimum singular values. The gain of $H$, expressed in terms of $\sigma_{\max}(Q)$, must be chosen to be smaller than this infimum. From inequality (14), the stability region will approach zero when the robot maneuvers near a singular point ($\det(J) \to 0$) and/or when the position gains approach infinity. Both cases are representative of "infinite stiffness" for the robot; the first is due to the robot configuration, while the second is due to the tracking controller.

## IV. Experimental Results

To evaluate the nonlinear stability condition, a compliance controller is implemented on a direct-drive three-degree-of-freedom robot [8], [9]. The University of Minnesota direct drive robot (Fig. 3) uses a four-bar linkage and is statically balanced without any counterweights. As a result of the elimination of the gravity forces, smaller actuators and, thus, smaller amplifiers were chosen to drive this robot. The motors yield acceleration of 5g at the endpoint without overheating. High-torque low-speed motors power the robot; specifically, the motors are neodymium (NdFeB) magnet AC brushless synchronous motors. Due to the high magnetic field strength (maximum energy products: 35 MGOe) of the rare earth NdFeB magnets, the motors have high torque-to-weight ratios. Pancake-type resolvers are used as position and velocity sensors. The peak torque of motors 1, 2, and 3 are 118 Nm, 78 Nm, and 58 Nm, respectively. The robot links are made of graphite-epoxy composite material. A microcomputer, which hosts a 4-node parallel processor with a PC/AT bus interface, is the main robot controller. Each node is an independent 32-bit processor with local memory and communication links to the other nodes in the system.

Because this robot has no gears, frictional losses are small and the manipulator can be modeled by equation (1). For a sufficient stability condition, if the condition is satisfied, stability is guaranteed; however, if the condition is violated, no conclusion can be made. Two experiments are performed to demonstrate that inequality (14) is a sufficient condition for stability: one experiment in which the satisfaction of the condition leads to a stable maneuver and one experiment in which parameters for an unstable maneuver violate the condition. In the first experiment, we design an $H$ such that inequality (14) is satisfied and show, through experiment, that the system is stable. In the second experiment, we show that an $H$ which destabilizes the system also violates inequality (14).

A reinforced aluminum wall is mounted vertically in the robot workspace, as shown in Fig. 3, to simulate a stiff environment. Fig. 4 shows the top view of the experimental setup. Motor 2 is mechanically locked, while motors 1 and 3 maneuver the robot endpoint horizontally. A piezoelectric force sensor is mounted on the manipulator endpoint to measure contact forces.

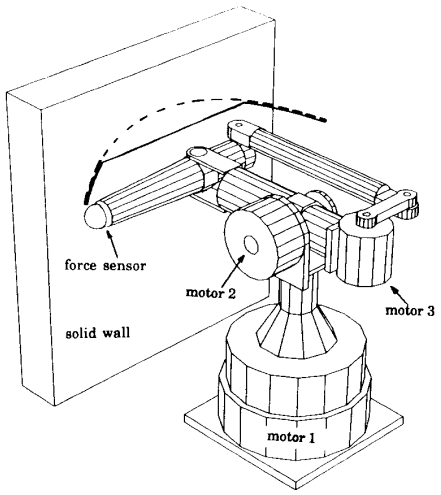


Fig. 4. The dashed line is the desired endpoint trajectory, while the solid line is the actual trajectory.

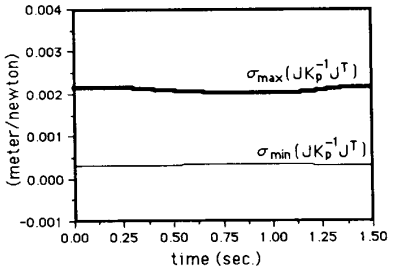


Fig. 5. The maximum and minimum singular values of the sensitivity function for the actual trajectory shown in Fig. 4.

Since the experiments are all two-dimensional, $H$ is a $2 \times 2$ matrix operating on contact forces which are normal and tangential to the wall. (The endpoint force measurements are resolved into the global coordinate frame.) In these experiments, only the compliancy in the direction normal to the wall is supplemented, so the following form of $H$ is chosen:

$$H = \begin{pmatrix} \frac{H_0}{Ts+1} & 0 \\ 0 & 0 \end{pmatrix} \tag{15}$$

where $T$ is an empirical constant and filters high-frequency noise in the force measurement. $T$ is fixed at 0.05 for all the experiments. The function, $r(t)$, shown in Fig. 4 by the dashed line, is the trajectory assigned to the robot. Since $H$ has only one nonzero member, then $\sigma_{max}(Q)$ will be the maximum value of the magnitude of $H_0/(Tj\omega + 1)$. The maximum value of $H$ is $H_0$ and occurs at dc ($\omega = 0$).

In the first experiment, we show that if inequality (14) is satisfied for a maneuver shown in Fig. 5, then the robot can have stable interaction with the environment. We choose $H_0$ to be 0.0003 so $H(s)$ is smaller than $\sigma_{min}(JK_p^{-1}J^T)$ for all configurations within the maneuver. Fig. 5 depicts $\sigma_{min}(JK_p^{-1}J^T)$ and $\sigma_{max}(JK_p^{-1}J^T)$ for the maneuver of Fig. 4. Fig. 6 shows the experimental and simulated values of the normal contact force. Stable contact is indicated by the absence of undamped oscillations in the normal force.

In the second experiment, $H_0$ is set to 0.0015. Fig. 7 shows the normal contact force as a function of time for experiment and simulation. In both results, the contact force oscillates throughout the maneuver, indicating that the compliance controller is unstable. Comparison with the singular value plot in Fig. 5 shows that $H_0$ exceeds the lower bound on $\sigma_{min}(JK_p^{-1}J^T)$; hence, the stability condition is violated. Since inequality (14) is a sufficient condition for stability, violation of this condition does not lead to any conclusion. The system can be stable even if the stability condition is not satisfied as in Fig. 8, which shows the experimental and simulated contact forces when $H_0 = 0.0005$.

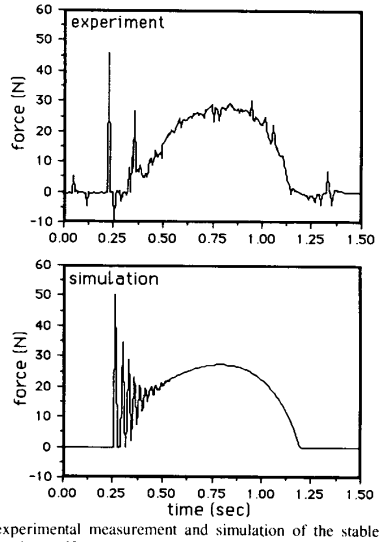


Fig. 6. The experimental measurement and simulation of the stable normal contact force. $H_0 = 0.0003$ satisfies the stability condition.

## V. Summary and Conclusion

An architecture for compliance control of direct drive robot manipulators is presented. The control approach allows not only tracking the input command vector in unconstrained space, but also compliancy in constrained maneuvers. A bound for the global stability of the robot and

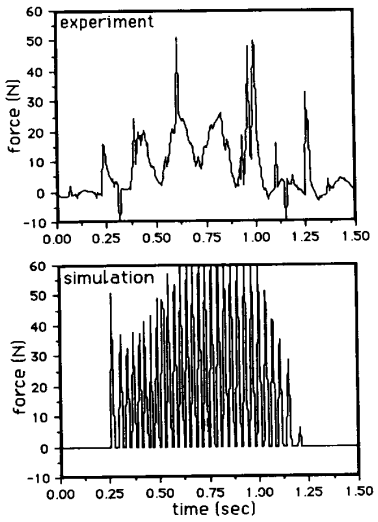


Fig. 7. The experimental measurement and simulation of the unstable normal contact force. $H_0 = 0.0015$ does not satisfy the stability condition.

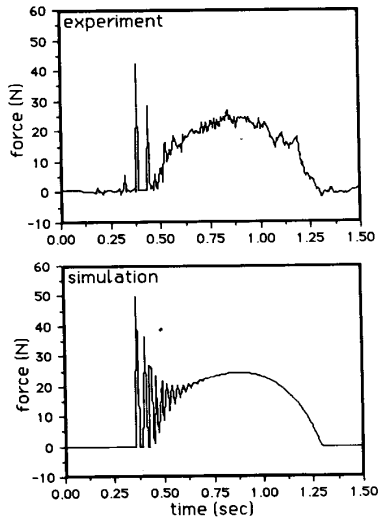


Fig. 8. The experimental measurement and simulation of the normal contact force. $H_0 = 0.0005$ violates the stability condition; however, the system is stable.

infinitely stiff environment, taken together, is derived. The stability region theoretically will approach zero when the robot maneuvers near its singular point and/or the position gain approaches infinity. Both cases are representative of infinite stiffness for the robot. Through both simulation and experimentation, the sufficiency of this condition is demonstrated.

## References

[1] C. H. An and J. M. Hollerbach, "Dynamic stability issues in force control of manipulators," in *Proc. IEEE Int. Conf. Robot. Automation*, Raleigh, NC, Mar. 1987, pp. 890–896.
[2] J. E. Colgate and N. Hogan, "Robust control of dynamically interacting systems," *Int. J. Contr.*, vol. 48, no. 1, July 1988.
[3] J. M. Hollerbach, "A recursive Lagrangian formulation of manipulator dynamics and a comparative study of dynamics formulation complexity," *IEEE Trans. Syst., Man, Cybern.*, vol. SMC-10, pp. 730–736, Nov. 1980.
[4] N. Hogan, "Impedance control: An approach to manipulation," *ASME J. Dynamic Syst., Meas., Contr.*, vol. 107, no. 1, pp. 1–24, Mar. 1985.
[5] —, "On the stability of manipulators performing contact tasks," presented at the Conf. Appl. Motion Contr., Minneapolis, MN, June 1987.
[6] H. Kazerooni, J. J. Bausch, and B. K. Kramer, "An approach to automated deburring by robot manipulators," *ASME J. Dynamic Syst., Meas., Contr.*, vol. 108, no. 4, Dec. 1986.
[7] H. Kazerooni, "Direct drive active compliant end-effector," *IEEE J. Robot. Automation*, vol. 4, June 1988.
[8] H. Kazerooni and S. Kim, "A new architecture for direct drive robots," in *Proc. IEEE Int. Conf. Robot. Automation*, vol. 1, Philadelphia, PA, Apr. 1988, pp. 442–445.
[9] H. Kazerooni, "Statically balanced direct drive robot manipulator," *Robotica*, vol. 7, no. 2, Apr. 1989.
[10] —, "Fundamentals of robust compliant motion for manipulators," *IEEE J. Robot. Automation*, vol. 2, June 1986.
[11] H. Kazerooni and T. I. Tsay, "On the stability of the constrained robotic maneuver," in *Proc. Amer. Contr. Conf.*, Atlanta, GA, June 1988, pp. 892–897.
[12] H. Kazerooni, "On the robot compliant motion control," *ASME J. Dynamic Syst., Meas., Contr.*, vol. 111, no. 3, Sept. 1989.
[13] H. Kazerooni, "Human–robot interaction via the transfer of power and information signals," *IEEE Trans. Syst., Man, Cybern.*, vol. 20, Mar. 1990.
[14] P. Lancaster, *Lambda-Matrices and Vibrating Systems*. Elmsford, NY: Pergamon, 1966.
[15] M. T. Mason, "Compliance and force control for computer controlled manipulators," *IEEE Trans. Syst., Man, Cybern.*, vol. SMC-11, pp. 418–432, June 1981.
[16] J. K. Mills and A. A. Goldenberg, "Force and position control of manipulators during constrained motion tasks," *IEEE Trans. Robot. Automation*, vol. 5, Feb. 1989.
[17] R. P. C. Paul and B. Shimano, "Compliance and control," in *Proc. Joint Automat. Contr. Conf.*, San Francisco, CA, 1976, pp. 694–699.
[18] M. H. Raibert and J. J. Craig, "Hybrid position force control of manipulators," *ASME J. Dynamic Syst., Meas., Contr.*, vol. 102, June 1981.
[19] K. J. Salisbury, "Active stiffness control of manipulator in Cartesian coordinates," in *Proc. 19th IEEE Conf. Decision Contr.*, Albuquerque, NM, Dec. 1980, pp. 95–100.
[20] M. W. Spong and M. Vidyasagar, "Robust nonlinear control of robot manipulators," presented at the IEEE Conf. Decision Contr., Dec. 1985.
[21] M. Vidyasagar, *Nonlinear Systems Analysis*. Englewood Cliffs, NJ: Prentice-Hall, 1978.
[22] M. Vidyasagar and C. A. Desoer, *Feedback Systems: Input-Output Properties*. New York: Academic, 1975.
[23] D. E. Whitney, "Force-feedback control of manipulator fine motions," *ASME J. Dynamic Syst., Meas., Contr.*, pp. 91–97, June 1977.
[24] —, "Historical perspective and state of the art in robot force control," *Int. J. Robot. Res.*, vol. 6, no. 1, Spring 1987.

# On the Problem of the Time-Optimal Manipulator Arm Turning

A. M. FORMAL SKY AND S. N. OSIPOV

*Abstract*—**This note is concerned with two kinds of manipulators making spatial movements. The problem of control which provides a manipulator turning in minimum possible time is considered. A control, satisfying the maximum principle of Pontryagin has been designed for some set of boundary configurations. With this control a manipulator link in the process of turning is oscillating around a position, corresponding to a minimum moment of inertia of a system with respect to an axis of rotation. Movement, satisfying the maximum principle, is compared to one for which the moment of inertia is minimal within the entire interval of time. The simplified equations as well as the complete ones are investigated.**

## Introduction

A rigid body can be turned around some axis more quickly if its moment of inertia is small with respect to that axis. When control of the manipulators is constructed, the problem of turning the system of rigid bodies arises. In addition to a turning angle, such a system has another controlled coordinate, and by varying it one can change a system mass

Manuscript received August 15, 1988; revised April 29, 1989.
The authors are with the Institute of Mechanics, Moscow University, Moscow, USSR.
IEEE Log Number 8934500.